Acta Geochim
DOI 10.1007/s11631-016-0131-5

ORIGINAL ARTICLE

Average iron isotopic compositions of the upper continental crust: constrained by loess from the Chinese Loess Plateau

Yingzeng Gong[1] · Ying Xia[1] · Fang Huang[1] · Huimin Yu[1]

Received: 22 September 2016 / Revised: 5 October 2016 / Accepted: 24 October 2016

Abstract Iron isotopic composition of the upper continental crust (UCC) is critical for understanding Fe mobilization and migration through the Earth. Because rocks exposed at Earth's surface have heterogeneous δ^{56}Fe, fine-grained clastic sediments can be used to estimate the average composition of UCC. In this study, we report δ^{56}Fe of loess-paleosol sequences from Yimaguan, Chinese Loess Plateau (CLP), to constrain the average Fe isotopic composition of UCC. The loess-paleosol sequences in this area formed in glacial-interglacial cycles and are characterized by varying degrees of weathering. Our data show that the loess-paleosol layers have extremely homogeneous Fe isotopic compositions with δ^{56}Fe ranging from +0.06‰ to +0.12‰, regardless of variations in the major element composition and weathering intensity. Our study indicates that since Fe isotopes are not significantly fractionated during loess deposition, the loess can be regarded as representative of UCC. It follows that the average δ^{56}Fe of UCC is 0.09‰ ± 0.03‰ (2SD), consistent with previous estimates based on igneous rock data.

Keywords Yimaguan · Loess · Fe isotopes · Upper continental crust

✉ Huimin Yu
huy16@ustc.edu.cn

[1] CAS Key Laboratory of Crust-Mantle Material and Environments, School of Earth and Space Sciences, University of Science and Technology of China, Hefei 230026, Anhui, China

1 Introduction

Iron is the most abundant metal element in the solar system, and the second most abundant element in the Earth and rocky planetary bodies (Wedepohl 1995; Rudnick and Gao 2003; Wang et al. 2012). Iron controls oxygen fugacity of the Earth from the core to the mantle and crust. As an indispensable element for a lot of important enzymes, Fe is an essential nutrient for organisms. Furthermore, in soils and water systems, Fe plays an important role in the transferability of nutrients and contaminants.

Iron exists as Fe^{3+}, Fe^{2+}, and Fe^{0} in nature. Iron isotopic compositions can be used to decipher the redox states and material cycle processes that have operated through geologic time (Weyer et al. 2007; Weyer and Ionov 2007; Dauphas et al. 2014). Furthermore, Fe isotopic compositions are an effective indicator of geosphere-biosphere cycles (Emmanuel et al. 2005; Guelke and von Blanckenburg 2007; Wiederhold et al. 2007a, b; Yesavage et al. 2012; Conway and John 2014; Poitrasson et al. 2014; Schuth et al. 2015). The Fe isotopic composition of the upper continental crust (UCC) is fundamental to tracing crustal material recycling and biogeochemical processes.

Iron isotopic compositions are defined as:

$$\delta^{x}\mathrm{Fe} = 1000 \times \left[\frac{\left(\frac{^{x}\mathrm{Fe}}{^{54}\mathrm{Fe}}\right)_{\mathrm{sample}}}{\left(\frac{^{x}\mathrm{Fe}}{^{54}\mathrm{Fe}}\right)_{\mathrm{standard}}} - 1 \right]$$

The international standard is IRMM-14 (produced by Institute for Reference Materials and Measurements, European Commission), with x as 56 or 57 reported by different authors. The relationship between δ^{56}Fe and δ^{57}Fe is $\delta^{56}\mathrm{Fe} = \delta^{57}\mathrm{Fe}/1.475$. Some studies report δ^{56}Fe

Published online: 26 November 2016

relative to the average of igneous rocks instead of IRMM-14; the two are related as follows:

$\delta^{56}Fe_{IRMM-14} = \delta^{56}Fe_{Igneousrocks} + 0.09‰$ (Beard and Johnson 2006).

Generally, the composition of UCC can be estimated by at least two methods (Rudnick and Gao 2003). One is to establish the weighted averages of the different types of rocks collected from UCC (Clarke 1889; Hu and Gao 2008); the other is based on the composition of fine-grained clastic sediment (e.g. shale, loess or glacial deposits) under the assumption that the sediment represents the average of a large area of continental crust (Goldschmidt 1933; Taylor and McLennan 1985; Beard and Johnson 2004; Teng et al. 2004; Poitrasson 2006; Hu and Gao 2008 Li et al. 2010).

Poitrasson (2006) reported that the average δ^{56}Fe of UCC is 0.08 ‰, assuming that δ^{56}Fe is homogenous in mafic rocks. However, additional data show that Fe isotopic fractionation during magmatic processes can reach ~1‰ due to crystallization, partial melting, and fluid exsolution (Zhu et al. 2001; Weyer et al. 2005; Weyer and Ionov 2007; Heimann et al. 2008; Teng et al. 2008; Schoenberg and von Blanckenburg 2006; Dauphas et al. 2009; Huang et al. 2011). Clearly, UCC has heterogeneous Fe isotopic composition (Fig. 3).

Beard and Johnson (2004) estimated the average δ^{56}Fe of UCC as 0.11‰ ± 0.1‰, based on the Fe isotopic compositions of clastic sedimentary rocks and suspended loads from rivers. Because Fe isotopes can be largely fractionated during weathering (Wiederhold et al. 2007a, b; Thompson et al. 2007; Guelke et al. 2010; Kiczka et al. 2011; Yesavage et al. 2012), the caculated result strongly depends on the coverage of samples. Therefore, the average δ^{56}Fe of UCC needs to be revisited.

Because fine-grained sediments or sedimentary rocks are generally formed by mechanical weathering and long-distance transport of continental rocks, they have been widely used to constrain the average composition of the UCC (e.g., Rudnick and Gao 2003; Park et al. 2012). The loess and paleosol of the Chinese Loess Plateau (CLP) originated from the Central Asian Orogenic Belt and the northern margin of the Tibetan plateau (Sun 2000, 2002; Sun et al. 2001, 2008; Li et al. 2007; Sun and Zhu 2010; Chen and Li 2011; Lu and Sun 2011; Wiederhold, 2015). Loess and paleosol samples from CLP have been used for estimating isotopic compositions (of Li, Cu, and Mg) of UCC due to limited chemical weathering (Teng et al. 2004; Li et al. 2009, 2010). During the loess-paleosol sequence formation, negligible Fe was chemically transported (Gu et al. 1997; Ding et al. 2001). Therefore, in this study, we analyzed the loess and paleosol samples from the loess-paleosol sequences (produced in glacial-interglacial cycles) of Yimaguan, located in the CLP near the classic profiles of Xifeng and Luochuan. The purpose of this study is to constrain Fe isotopic compositions of UCC.

2 Samples and methods

2.1 Sample descriptions

In order to constrain the Fe isotopic composition of UCC, 15 loess and 17 paleosol samples were collected from Yimaguan, Gansu Province, China (35°55′N, 107°37′E) (Fig. 1) (Hao et al. 2012). The depth of the profile ranges from 0 to 31 m. The loess(L)-paleosol(S) sequence from top to bottom is S0, L1, S1, L2, S2, L3 (Fig. 2). The sequence formed in a drastically different climate. The frequency-dependent magnetic susceptibility (χ_{fd}) of loess in the CLP is a well-accepted proxy for summer and winter monsoon climates (Ryu et al. 2011; Hao et al. 2012; Eiler et al. 2014; Da et al. 2015; Gontier et al. 2015; Sauzéat et al. 2015; Teitler et al. 2015). The χ_{fd} values of this sequence have been presented in Hao et al. (2012). The

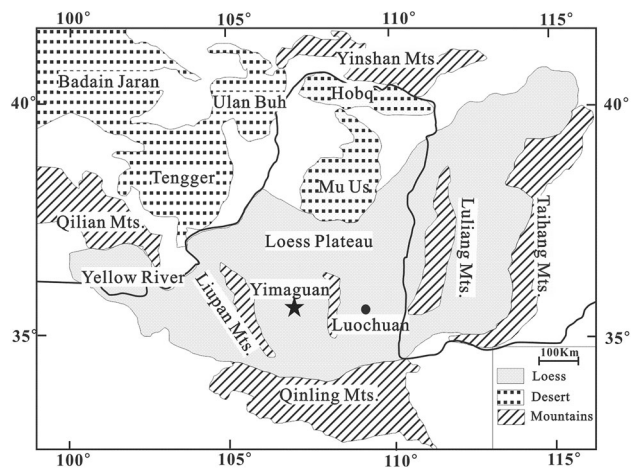

Fig. 1 Location of the Yimaguan section (from Sun 2002)

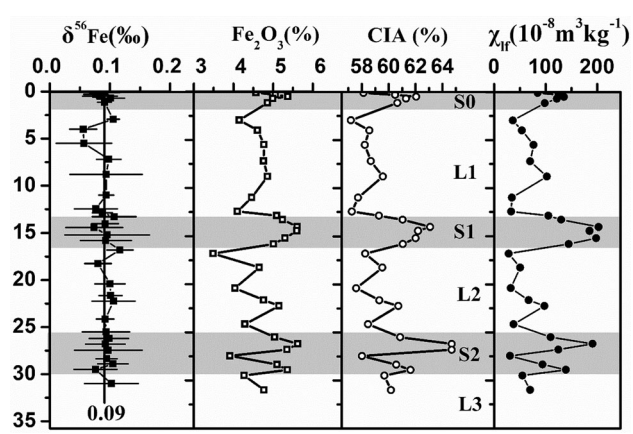

Fig. 2 The δ^{56}Fe, Fe/Ti, CIA, and χ_{fd} values of bulk loess-paleosol samples in the Yimaguan section. The grey bars marked S0, S1, and S2 represent the paleosol layers; L1, L2, and L3 show the loess layers

high-χ_{fd} layers (paleosol) deposited during weaker winter monsoon and stronger summer monsoon are characterized by more pronounced weathering, and the low χ_{fd} values (in loess) display weaker weathering (Ryu et al. 2011; Hao et al. 2012; Eiler et al. 2014; Da et al. 2015; Gontier et al. 2015; Sauzéat et al. 2015; Teitler et al. 2015).

2.2 Analytical methods

2.2.1 Major element analyses

Major element contents were analyzed using X-ray fluorescence spectroscopy with an AXIOS Minerals spectrometer (produced by PANalytical) at the Institute of Geology and Geophysics, Chinese Academy of Sciences. The relative standard deviation in this laboratory is less than 1%.

2.2.2 Fe isotopic composition analyses

Bulk samples were ground to powder in an agate mortar after being air dried. Approximately 15 mg of sample powder was weighed into acid-washed Savillex vials. The organic matter in the sample was repeatedly decomposed by a mixture of 1 mL HNO_3 (15 mol/L) and 1 mL H_2O_2 (30%) until the organic matter was completely broken down. After being evaporated to dryness, the sample was further digested by a mixture of 1 mL HNO_3 (15 mol/L)

Table 1 The major element contents (wt%) in the loess-paleosol profile

Sample name	SiO_2	TiO_2	Al_2O_3	TFe_2O_3	MnO	MgO	CaO	Na_2O	K_2O	P_2O_5	Fe/Ti	CIA (%)
111-XF2-4	63.0	0.7	12.3	4.6	0.1	2.2	5.8	1.9	2.5	0.2	8.6	58.1
111-XF2-12	67.5	0.7	13.7	5.1	0.1	1.9	1.8	1.9	2.6	0.1	9.0	60.5
111-XF2-20	66.1	0.7	14.1	5.4	0.1	2.0	1.7	1.8	2.7	0.1	9.5	62.0
111-XF2-28	63.1	0.7	13.2	5.0	0.1	1.9	3.1	1.7	2.5	0.1	9.3	61.3
111-XF2-46	62.1	0.7	12.9	4.9	0.1	2.0	5.6	1.7	2.5	0.2	9.2	60.6
10XF-110	60.5	0.6	11.3	4.2	0.1	2.2	8.4	1.8	2.3	0.1	8.7	57.2
10XF-152	59.6	0.6	12.2	4.6	0.1	2.3	7.2	1.8	2.5	0.2	9.2	58.6
10XF-212	59.1	0.7	12.5	4.8	0.1	2.3	7.8	1.8	2.7	0.2	9.2	58.2
10XF-280	59.0	0.7	12.4	4.8	0.1	2.3	7.9	1.8	2.7	0.2	9.4	58.7
10XF-344	58.7	0.7	12.6	4.9	0.1	2.2	7.6	1.7	2.7	0.2	9.4	59.6
10XF-432	57.4	0.6	11.7	4.5	0.1	2.3	9.2	1.8	2.5	0.1	9.1	57.7
10XF-490	56.9	0.6	11.0	4.1	0.1	2.3	10.5	1.7	2.3	0.1	8.8	57.3
10XF-527	61.2	0.7	13.1	5.1	0.1	2.4	4.8	1.9	2.6	0.1	9.5	59.3
10XF-545	61.3	0.7	13.4	5.2	0.1	2.4	5.4	1.7	2.6	0.2	9.4	61.0
10XF-574	65.6	0.8	14.6	5.6	0.1	2.4	1.5	1.9	2.8	0.2	9.4	63.1
10XF-590	66.5	0.8	14.6	5.6	0.1	2.3	1.3	2.4	2.8	0.2	9.4	62.2
10XF-623	64.0	0.7	13.8	5.3	0.1	2.2	3.8	1.7	2.6	0.1	9.3	62.0
10XF-646	67.3	0.7	13.7	5.0	0.1	2.2	2.2	1.8	2.6	0.1	8.9	61.0
10XF-682	51.2	0.5	9.8	3.5	0.1	1.8	12.0	1.5	1.9	0.1	8.4	58.3
10XF-742	59.0	0.6	12.2	4.7	0.1	2.4	7.7	1.7	2.4	0.1	9.3	59.5
10XF-826	58.6	0.6	11.0	4.0	0.1	2.2	9.6	1.7	2.2	0.1	8.8	57.6
10XF-878	60.2	0.7	12.5	4.8	0.1	2.4	6.6	1.8	2.5	0.1	9.1	59.3
10XF-902	63.5	0.7	13.6	5.2	0.1	2.4	4.7	1.8	2.7	0.1	9.1	60.7
10XF-978	57.1	0.6	11.3	4.3	0.1	2.3	9.8	1.7	2.3	0.1	8.9	58.5
10XF-1028	61.1	0.7	13.1	5.0	0.1	2.4	6.2	1.7	2.6	0.1	9.3	60.9
10XF-1060	66.6	0.8	14.6	5.6	0.1	2.2	1.3	1.7	2.8	0.1	9.3	64.7
10XF-1084	67.8	0.7	14.2	5.4	0.1	2.2	1.2	1.9	2.7	0.1	9.3	64.7
10XF-1110	56.4	0.6	10.6	3.9	0.1	2.0	11.1	1.6	2.1	0.1	8.7	58.0
10XF-1146	62.8	0.7	13.3	5.1	0.1	2.3	4.8	1.8	2.6	0.1	9.3	60.6
10XF-1168	64.4	0.7	13.9	5.4	0.1	2.2	2.8	1.7	2.7	0.1	9.4	61.6
10XF-1192	55.3	0.6	11.2	4.3	0.1	2.1	11.4	1.6	2.2	0.1	9.1	59.7
10XF-1252	58.9	0.7	12.4	4.8	0.1	2.3	7.6	1.7	2.5	0.2	9.2	60.2

CIA are calculated following the measurements of McLennan (1993)

and 3 mL HF (24 mol/L) followed by evaporation in a mixture of 1 mL HNO_3 (15 mol/L) and 3 mL HCl (11 mol/L). Finally, the sample was dissolved in 6 mol/L HC for chromatography.

Samples were purified using 0.5 mL anion resin (Bio-Rad, AG1-X8, 200–400 mesh). Matrix elements were leached by 4 mL 6-mol/L HCl and Fe was consequently collected in 4 mL 0.4-mol/L HCl, 1 ml 8-mol/L HCl, and 0.5 ml H_2O. The whole procedural blank for Fe was <20 ng, which is negligible compared with the amount of Fe (50 μg) loaded on the column. The recovery of the procedure was >99%.

The Fe isotopes were measured by the sample-standard bracketing (SSB) method using Thermo Scientific Neptune plus MC-ICP-MS in the CAS Key Laboratory of Crust-Mantle Material and Environments, University of Science and Technology of China (USTC in Hefei, Anhui Province). Measurements were run at high-resolution mode ($M/\Delta M = \sim 8900$) with Jet sampling cone and Ni H-skimmer cone. The partially resolved Fe peak with flat-topped shoulder on the left side was chosen to avoid the effect of molecular interference (mainly $^{40}Ar^{16}O$). The long-term external precision of $\delta^{56}Fe$ was monitored by analyses of the high-purity Fe solutions of UIFe ($\delta^{56}Fe = 0.688‰ \pm 0.048$ ‰, n = 1219, 2SD) and GSB-1 ($\delta^{56}Fe = 0.719‰ \pm 0.046$ ‰, n= 771, 2SD) for 20 months, and found to be better than ±0.050‰. We measured BHVO-2 as 0.09‰ ± 0.04‰ (n = 3) and the duplicate one as 0.06‰ ± 0.05‰ (n = 3), which are indistinguishable to the reference value reported in Craddock and Dauphas (2011) (0.11‰ ± 0.03‰) within error. We also analyzed the Certified Reference Materials for the Chemical Composition of Soil of China GBW07454 from Luochuan, which is another classic loess section of CLP approximately 160 km east of the Yimaguan profile.

3 Results

The $\delta^{56}Fe$ values of the profile are presented in Table 1 and Fig. 2. Chemical index of alteration (CIA) was calculated following McLennan (1993). χ_{fd} values are from Hao et al. (2012). Our data show synchronous variations in Fe, CIA, and χ_{fd}. However, $\delta^{56}Fe$ values are homogenous in both high- and low-χ_{fd} samples (Hao et al. 2012), ranging from +0.06 to +0.12‰ with an average at 0.09‰ (Table 2). The $\delta^{56}Fe$ of GBW07454 (loess standard from Luochuan, China) is consistent with the value of samples from Yimaguan, possibly implying homogeneous Fe isotopes in Yimaguan and Luochuan. In comparison to igneous rock with heterogeneous Fe isotopic compositions, the loess-paleosol samples are better candidates for representing the Fe isotopic compositions of UCC.

4 Discussion

Homogeneous $\delta^{56}Fe$ in the loess-paleosol sequences may be due to negligible Fe transference or no isotope fractionation during Fe transference. The remarkable difference in the content of Fe in the loess-paleosol sequence (Fig. 2) is due to the variation of $CaCO_3$ (Diao and Wen 1997). In the paleosol layers, the high content of Fe is due to the heavy loss of the carbonate. Besides in silicate, Fe can be conserved as oxide (such as magnetite, maghmite, and hematite), hydroxide (goethite, lepidocrocite), or sulfide (pyrrhotite, pyrite, and greigite) in loess and paleosol. Although the loess and paleosol formed under different climates, both were produced under weakly oxidizing and alkaline conditions. In the loess-paleosol sequence, Fe can be stably conserved in different compositions of iron-bearing minerals. Additionally, previous studies show that the loess-paleosol sequences in the CLP are subjected to weathering processes which leach Na and Ca (Fig. 2) with negligible transference of Fe (Gu et al. 1997; Ding et al. 2001) (Fig. 3).

During weathering, the Fe^{2+} with lighter $\delta^{56}Fe$ value is transferred preferentially over Fe^{3+} (Wiederhold et al. 2007a; Schuth et al. 2015; Veenstra and Lee 2015). The Fe bonded by organic matter is enriched in ^{54}Fe and is fluid-mobile (Emmanuel et al., 2005; Guelke and von Blanckenburg 2007; Wiederhold et al. 2007b). Overall, ^{54}Fe is lost preferencially compared to ^{56}Fe (Wiederhold et al., 2007a; Thompson et al. 2007; Guelke et al. 2010; Kiczka et al. 2011; Yesavage et al. 2012). However, the homogeneous $\delta^{56}Fe$ in the loess-paleosol sequence reveals that there is no obvious fractionation during erosion, transference, sedimentation, and soil formation. This means that the $\delta^{56}Fe$ in the loess-paleosol sequence can well represent the value of the source rock.

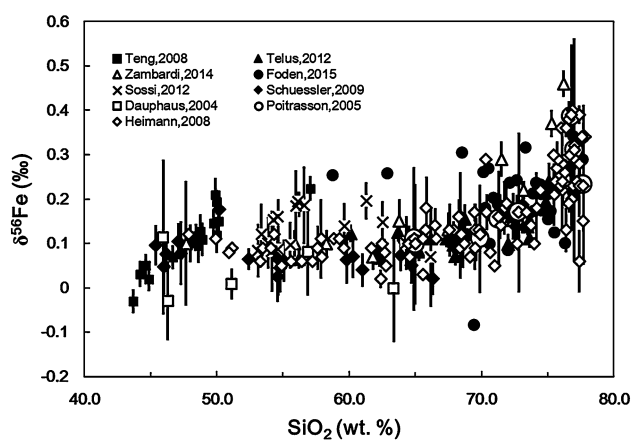

Fig. 3 The $\delta^{56}Fe$ variations in igneous rocks. Data sources: Dauphas et al. (2004), Poitrasson and Freydier (2005), Heimann et al. (2008), Teng et al. (2008), Schuessler et al. (2009), Sossi et al. (2012), Telus et al. (2012), Zambardi et al. (2014), Foden et al. (2015)

Table 2 The Fe isotopic compositions of the samples

Samples	Depth (m)	δ^{56}Fe	2SD	n
111-XF2-4	0.10	0.09	0.03	3
111-XF2-12	0.30	0.08	0.02	3
111-XF2-20	0.50	0.08	0.03	3
111-XF2-28	0.70	0.10	0.02	3
111-XF2-46	1.15	0.09	0.01	3
10XF-110	2.95	0.11	0.01	3
10XF-152	4.00	0.06	0.02	3
10XF-212	5.50	0.06	0.05	3
10XF-280	7.20	0.10	0.02	3
10XF-344	8.80	0.09	0.06	3
Repeated	8.80	0.06	0.04	3
10XF-432	11.00	0.09	0.01	3
10XF-490	12.45	0.08	0.04	3
10XF-527	12.88	0.09	0.02	3
10XF-545	13.30	0.11	0.04	3
10XF-574	14.05	0.09	0.02	3
10XF-590	14.45	0.07	0.05	3
10XF-623	15.20	0.10	0.07	3
10XF-646	15.80	0.09	0.04	2
10XF-682	16.80	0.12	0.02	2
10XF-742	18.25	0.08	0.02	3
10XF-826	20.40	0.10	0.02	3
10XF-878	21.65	0.10	0.02	3
10XF-902	22.25	0.11	0.04	3
10XF-978	24.15	0.09	0.01	3
10XF-1028	25.50	0.09	0.04	3
10XF-1060	26.20	0.10	0.03	3
10XF-1084	26.80	0.09	0.03	3
10XF-1110	27.45	0.10	0.06	3
10XF-1146	28.35	0.09	0.02	3
Repeated	28.35	0.07	0.01	3
10XF-1168	28.90	0.10	0.03	3
10XF-1192	29.50	0.08	0.04	3
10XF-1252	31.00	0.10	0.04	3
GBW07454		0.07	0.05	3
Repeated		0.09	0.03	3
BHVO-2		0.09	0.04	3
Repeated		0.06	0.05	3
Reference*		0.11	0.03	12

GBW07454 is the national soil reference material of China (loess from Luochuan in the middle of the CLP). *The reference value reported in Craddock and Dauphas (2011). "n" denotes the number of Fe isotope analyses

Fine-grained clastic sedimentary rocks (e.g., shale) or loess and glacial deposits were previously used to derive the average upper crustal composition for insoluble elements, such as Th and Ti (Goldschmidt 1933; Taylor and McLennan 1985; Rudnick and Gao 2003; Teng et al. 2004; Hu and Gao 2008; Li et al. 2009, 2010). Our data show that the Fe isotopic compositions of bulk rocks from the CLP are homogeneous and represent the character of the original source matter mixing from a large area. Considering the large Fe isotopic heterogeneity of igneous rocks, the loess-paleosol sequence is a better candidate for estimating Fe isotopic compositions of UCC.

5 Conclusion

Based on the weighted average of loess-paleosol samples from the CLP, we constrain the δ^{56}Fe value of the UCC at 0.09‰ ± 0.03‰ (2SD). Although our estimate is indistinguishable from the value given by Poitrasson (2006) (0.08‰) and Beard and Johnson (2004) (0.11‰), our new estimate provides a more refined value. The Fe isotopic composition of UCC is heavier than that of the upper mantle (Weyer and Ionov 2007) and of bulk Earth (Dauphas et al. 2009), suggesting Fe isotopic fractionation during crustal formation and evolution.

Acknowledgements This research was financially supported by the National Science Foundation of China (41173031, 41325011 and 41503001), and the Fundamental Research Funds for the Central Universities (WK3410000004). We are grateful to Dr. Qingzhen Hao for providing the samples.

References

Beard BL, Johnson CM (2004) Fe isotope variations in the modern and ancient earth and other planetary bodies. Rev Mineral Geochem 55(1):319–357

Beard BL, Johnson CM (2006) Comment on "heavy iron isotope composition of granites determined by high resolution mc-icp-ms", by f. Poitrasson and r. Freydier [chem. Geol. 222 132–147]. Chem Geol 235(1–2):201–204

Chen J, Li G (2011) Geochemical studies on the source region of Asian dust. Sci China Earth Sci 54(9):1279–1301

Clarke FW (1889) The relative abundance of the chemical elements. Philos Soc Wash Bull X. 1:131–142

Conway TM, John SG (2014) Quantification of dissolved iron sources to the North Atlantic Ocean. Nature 511(7508):212–215

Craddock PR, Dauphas N (2011) Iron isotopic compositions of geological reference materials and chondrites. Geostand Geoanal Res 35(1):101–123

Da J, Zhang YG, Wang H, Balsam W, Ji J (2015) An early pleistocene atmospheric CO_2 record based on pedogenic carbonate from the Chinese loess deposits. Earth Planet Sci Lett 426:69–75

Dauphas N, van Zuilen M, Wadhwa M, Davis AM, Marty B, Janney PE (2004) Clues from Fe isotope variations on the origin of early archean bifs from Greenland. Science 306(5704):2077–2080

Dauphas N, Craddock PR, Asimow PD, Bennett VC, Nutman AP, Ohnenstetter D (2009) Iron isotopes may reveal the redox conditions of mantle melting from archean to present. Earth Planet Sci Lett 288(1–2):255–267

Dauphas N, Roskosz M, Alp EE, Neuville DR, Hu MY, Sio CK, Tissot FLH, Zhao J, Tissandier L, Médard E, Cordier C (2014) Magma redox and structural controls on iron isotope variations in earth's mantle and crust. Earth Planet Sci Lett 398:127–140

Diao G, Wen Q (1997) The paleoclimatic variation records of carbonate and iron oxides in the weinan loess section. Chin J Geochem 16(1):62–68

Ding ZL, Yang SL, Sun JM, Liu TS (2001) Iron geochemistry of loess and red clay deposits in the Chinese loess plateau and implications for long-term Asian monsoon evolution in the last 7.0 Ma. Earth Planet Sci Lett 185(1–2):99–109

Eiler JM, Bergquist B, Bourg I, Cartigny P, Farquhar J, Gagnon A, Guo W, Halevy I, Hofmann A, Larson TE, Levin N, Schauble EA, Stolper D (2014) Frontiers of stable isotope geoscience. Chem Geol 372:119–143

Emmanuel S, Erel Y, Matthews A, Teutsch N (2005) A preliminary mixing model for Fe isotopes in soils. Chem Geol 222(1–2):23–34

Foden J, Sossi PA, Wawryk CM (2015) Fe isotopes and the contrasting petrogenesis of a-, i- and s-type granite. Lithos 212–215:32–44

Goldschmidt V (1933) Grundlagen der quantitativen geochemie. Fortschr Mineral Krist Petrog 17(1):12

Gontier A, Rihs S, Chabaux F, Lemarchand D, Pelt E, Turpault M-P (2015) Lack of bedrock grain size influence on the soil production rate. Geochim Cosmochim Acta 166:146–164

Gu ZY, Lal D, Liu TS, Guo ZT, Southon J, Caffee MW (1997) Weathering histories of Chinese loess deposits based on uranium and thorium series nuclides and cosmogenic 10be. Geochim Cosmochim Acta 61(24):5221–5231

Guelke M, von Blanckenburg F (2007) Fractionation of stable iron isotopes in higher plants. Environ Sci Technol 41(6):1896–1901

Guelke M, von Blanckenburg F, Schoenberg R, Staubwasser M, Stuetzel H (2010) Determining the stable Fe isotope signature of plant-available iron in soils. Chem Geol 277(3–4):269–280

Hao Q, Wang L, Oldfield F, Peng S, Qin L, Song Y, Xu B, Qiao Y, Bloemendal J, Guo Z (2012) Delayed build-up of arctic ice sheets during 400,000 year minima in insolation variability. Nature 490(7420):393–396

Heimann A, Beard BL, Johnson CM (2008) The role of volatile exsolution and sub-solidus fluid/rock interactions in producing high $^{56}Fe/^{54}Fe$ ratios in siliceous igneous rocks. Geochim Cosmochim Acta 72(17):4379–4396

Hu Z, Gao S (2008) Upper crustal abundances of trace elements: a revision and update. Chem Geol 253(3–4):205–221

Huang F, Zhang Z, Lundstrom CC, Zhi X (2011) Iron and magnesium isotopic compositions of peridotite xenoliths from eastern China. Geochim Cosmochim Acta 75(12):3318–3334

Kiczka M, Wiederhold JG, Frommer J, Voegelin A, Kraemer SM, Bourdon B, Kretzschmar R (2011) Iron speciation and isotope fractionation during silicate weathering and soil formation in an alpine glacier forefield chronosequence. Geochim Cosmochim Acta 75(19):5559–5573

Li G, Chen J, Chen Y, Yang J, Ji J, Liu L (2007) Dolomite as a tracer for the source regions of Asian dust. J Geophys Res 112(D17):D17201

Li W, Jackson SE, Pearson NJ, Alard O, Chappell BW (2009) The Cu isotopic signature of granites from the lachlan fold belt, SE Australia. Chem Geol 258(1–2):38–49

Li W-Y, Teng F-Z, Ke S, Rudnick RL, Gao S, Wu F-Y, Chappell BW (2010) Heterogeneous magnesium isotopic composition of the upper continental crust. Geochim Cosmochim Acta 74(23):6867–6884

Lu T, Sun J (2011) Luminescence sensitivities of quartz grains from eolian deposits in Northern China and their implications for provenance. Quat Res 76(2):181–189

McLennan SM (1993) Weathering and global denudation. J Geol 101(2):295–303

Milliman JD, Meade RH (1983) World-wide delivery of river sediment to the oceans. J Geol 91(1):1–21

Park J-W, Hu Z, Gao S, Campbell IH, Gong H (2012) Platinum group element abundances in the upper continental crust revisited – new constraints from analyses of Chinese loess. Geochim Cosmochim Acta 93:63–76

Poitrasson F (2006) On the iron isotope homogeneity level of the continental crust. Chem Geol 235(1–2):195–200

Poitrasson F, Freydier R (2005) Heavy iron isotope composition of granites determined by high resolution mc-icp-ms. Chem Geol 222(1–2):132–147

Poitrasson F, Cruz Vieira L, Seyler P, dos Santos Márcia, Pinheiro G, Santos Mulholland D, Bonnet M-P, Martinez J-M, Alcantara Lima B, Resende Boaventura G, Chmeleff J, Dantas EL, Guyot J-L, Mancini L, Martins Pimentel M, Ventura Santos R, Sondag F, Vauchel P (2014) Iron isotope composition of the bulk waters and sediments from the Amazon River basin. Chem Geol 377:1–11

Rudnick R, Gao S (2003) Composition of the continental crust. Treatise Geochem 3:1–64

Ryu J-S, Jacobson AD, Holmden C, Lundstrom C, Zhang Z (2011) The major ion, δ44/40ca, δ44/42ca, and δ26/24 mg geochemistry of granite weathering at ph = 1 and t = 25°c: power-law processes and the relative reactivity of minerals. Geochim Cosmochim Acta 75(20):6004–6026

Sauzéat L, Rudnick RL, Chauvel C, Garçon M, Tang M (2015) New perspectives on the li isotopic composition of the upper continental crust and its weathering signature. Earth Planet Sci Lett 428:181–192

Schoenberg R, von Blanckenburg F (2006) Modes of planetary-scale Fe isotope fractionation. Earth Planet Sci Lett 252(3–4):342–359

Schuessler JA, Schoenberg R, Sigmarsson O (2009) Iron and lithium isotope systematics of the Hekla volcano, Iceland — evidence for Fe isotope fractionation during magma differentiation. Chem Geol 258(1–2):78–91

Schuth S, Hurraß J, Münker C, Mansfeldt T (2015) Redox-dependent fractionation of iron isotopes in suspensions of a groundwater-influenced soil. Chem Geol 392:74–86

Sossi PA, Foden JD, Halverson GP (2012) Redox-controlled iron isotope fractionation during magmatic differentiation: an example from the red hill intrusion, s. Tasmania. Contrib Mineral Petrol 164(5):757–772

Sun J (2000) Origin of eolian sand mobilization during the past 2300 years in the Mu US desert, China. Quat Res 53(1):78–88

Sun J (2002) Provenance of loess material and formation of loess deposits on the Chinese loess plateau. Earth Planet Sci Lett 203(3–4):845–859

Sun J, Zhu X (2010) Temporal variations in pb isotopes and trace element concentrations within Chinese eolian deposits during the past 8 Ma: implications for provenance change. Earth Planet Sci Lett 290(3–4):438–447

Sun J, Zhang M, Liu T (2001) Spatial and temporal characteristics of dust storms in China and its surrounding regions, 1960–1999: relations to source area and climate. J Geophys Res 106(D10):10325

Sun J, Zhang L, Deng C, Zhu R (2008) Evidence for enhanced aridity in the Tarim basin of China since 5.3 Ma. Quat Sci Rev 27(9–10):1012–1023

Taylor SR, McLennan SM (1985) The continental crust: its composition and evolution. Blackwell,Oxford, 312 pp.

Teitler Y, Philippot P, Gérard M, Le Hir G, Fluteau F, Ader M (2015) Ubiquitous occurrence of basaltic-derived paleosols in the Late Archean Fortescue Group, Western Australia. Precambr Res 267:1–27

Telus M, Dauphas N, Moynier F, Tissot FLH, Teng F-Z, Nabelek PI, Craddock PR, Groat LA (2012) Iron, zinc, magnesium and uranium isotopic fractionation during continental crust differentiation: the tale from migmatites, granitoids, and pegmatites. Geochim Cosmochim Acta 97:247–265

Teng FZ, McDonough WF, Rudnick RL, Dalpé C, Tomascak PB, Chappell BW, Gao S (2004) Lithium isotopic composition and concentration of the upper continental crust. Geochim Cosmochim Acta 68(20):4167–4178

Teng F-Z, Dauphas N, Helz RT (2008) Iron isotope fractionation during magmatic differentiation in kilauea iki lava lake. Science 320(5883):1620–1622

Thompson A, Ruiz J, Chadwick OA, Titus M, Chorover J (2007) Rayleigh fractionation of iron isotopes during pedogenesis along a climate sequence of hawaiian basalt. Chem Geol 238(1–2): 72–83

Veenstra JJ, Lee Burras C (2015) Soil profile transformation after 50 years of agricultural land use. Soil Sci Soc Am J 79(4):1154

Wang K, Moynier F, Dauphas N, Barrat J-A, Craddock P, Sio CK (2012) Iron isotope fractionation in planetary crusts. Geochim Cosmochim Acta 89:31–45

Wedepohl KH (1995) The composition of the continental crust. Geochim Cosmochim Acta 59(7):1217–1232

Weyer S, Ionov DA (2007) Partial melting and melt percolation in the mantle: the message from Fe isotopes. Earth Planet Sci Lett 259(1–2):119–133

Weyer S, Anbar AD, Brey GP, Münker C, Mezger K, Woodland AB (2007) Fe-isotope fractionation during partial melting on earth and the current view on the Fe-isotope budgets of the planets (reply to the comment of f. Poitrasson and to the comment of b.L. Beard and c.M. Johnson on "iron isotope fractionation during planetary differentiation" by s. Weyer, a.D. Anbar, g.P. Brey, c. Münker, k. Mezger and a.B. Woodland). Earth Planet Sci Lett 256(3–4):638–646

Wiederhold JG (2015) Metal stable isotope signatures as tracers in environmental geochemistry. Environ Sci Technol 49(5): 2606–2624

Wiederhold JG, Teutsch N, Kraemer SM, Halliday AN, Kretzschmar R (2007a) Iron isotope fractionation during pedogenesis in redoximorphic soils. Soil Sci Soc Am J 71(6):1840

Wiederhold JG, Teutsch N, Kraemer SM, Halliday AN, Kretzschmar R (2007b) Iron isotope fractionation in oxic soils by mineral weathering and podzolization. Geochim Cosmochim Acta 71(23):5821–5833

Yesavage T, Fantle MS, Vervoort J, Mathur R, Jin L, Liermann LJ, Brantley SL (2012) Fe cycling in the shale hills critical zone observatory, Pennsylvania: an analysis of biogeochemical weathering and Fe isotope fractionation. Geochim Cosmochim Acta 99:18–38

Zambardi T, Lundstrom CC, Li X, McCurry M (2014) Fe and Si isotope variations at Cedar Butte Volcano; insight into magmatic differentiation. Earth Planet Sci Lett 405:169–179

Zhu XK, Guo Y, O'Nions RK, Young ED, Ash RD (2001) Isotopic homogeneity of iron in the early solar nebula. Nature 412(6844):311–313